Westerduinweg 3
1755 LE Petten
P.O. Box 15
1755 ZG Petten
The Netherlands

www.tno.nl

T +31 88 866 50 65

TNO report

TNO 2018 R11428 | Final report

Observational Analyses of the North Sea Low-Level Jet

Date	26 November 2018
Author(s)	J.B. Duncan
Copy no	
No. of copies	
Number of pages	225
Number of appendices	0
Sponsor	Supported with Topsector Energy Subsidy from the Ministry of Economic Affairs and Climate Policy
Project name	Dutch Offshore Wind Atlas (DOWA)
Project number	060.33810

STummary

As part of the Dutch Offshore Wind Atlas (DOWA) project, analyses were performed on offshore wind measurements to provide enhanced characterisation of the North Sea wind climate. Of particular interest was the spatiotemporal behaviour of the offshore low-level jet (LLJ) – an anomalous wind event that can significantly impact both wind turbine power performance and loading. LLJs are characterised by a maximum in the vertical wind speed profile relatively close to the surface. LLJ frequency, vertical wind profile characteristics, and onset mechanisms have been extensively studied onshore. However, accurate measurement of the offshore wind environment at high altitudes (i.e. above typical mast heights [~100 m]) has historically been limited. Therefore, less is known regarding the behaviour of the offshore LLJ. Recent emphasis on offshore wind measurement by the Dutch Ministry of Economic Affairs has prompted the installation of high-quality anemometry on platforms distributed throughout the North Sea. Including both meteorological masts and light detection and ranging (lidar) units, these measurement systems enable accurate measurement of atmospheric boundary layer (ABL) winds at high altitudes, thereby increasing researcher ability to study anomalous wind behaviour offshore. Within this study, wind data from seven different North Sea measurement platforms – including several located within wind farm zones – were analysed to investigate North Sea LLJ behaviour.

LLJ frequency was examined in this study using identification criteria established by Baas et al. (2009). At MMIJ, a LLJ wind profile was detected 3.87 % of the time with the LLJ maxima occurring on average at 101.51 m with a mean wind speed of 9.28 m s^{-1}. LLJ frequency and LLJ maxima height and strength varied between measurement locations, but also depended heavily upon both seasonal cycle and the site-relative measurement height and vertical sampling range. At MMIJ, LLJ frequency increased to 7.56 % during the summer and 6.61 % during the spring. Whereas during the fall and winter, MMIJ LLJ frequency was significantly reduced. Measurement sites that sampled the ABL wind field across a greater vertical range and at higher heights typically detected a larger number of LLJs, as well as higher mean values of LLJ maxima height and wind speed. A novel method was also established in this study to systematically define LLJ events so that LLJ temporal behaviour (i.e. onset time and duration) could be quantitatively examined. LLJ events typically initiated during the night at MMIJ and persisted for an average duration of 96.6 min. However, the LLJ event duration distribution was heavy-tailed (positive skew), with several LLJ events lasting in excess of 10 hrs. Despite exhibiting seasonal dependencies, LLJ duration did not significantly differ between sites – unlike LLJ frequency and LLJ maxima height and strength.

Despite impediments to direct inter-site comparison (i.e. variations in site-measurement height and seasonal data availability), techniques were established to explore on a first-order basis North Sea LLJ spatial coherence. Research demonstrated that if a LLJ were detected at a given measurement site, there was a high likelihood (> 70 %) that a LLJ wind profile would also be detected at a neighbouring measurement site within a 24-hr period. This supports prior research that LLJs are not spatially isolated events, but rather can occupy significant spatial areas.

Contents

1 Introduction

The Dutch Part of the North Sea is expected to see substantial growth in offshore wind energy over the next decade. By 2023, the Dutch Part of the North Sea should have a total installed capacity of 4.5 GW, and by 2030 an installed capacity of 11.5 GW. Efficient development of offshore wind energy requires a thorough understanding of offshore wind conditions – including both mean state and anomalous behaviour. Numerical wind models can reasonably depict mean wind state. However, anomalous wind conditions are less understood and often insufficiently resolved within numerical models (Brown et al. 2005; Mirocha et al. 2016) – in part because offshore wind measurements are historically limited. Anomalous wind events have the potential to significantly impact wind turbine power performance and loading (Burton et al. 2011; Park et al. 2014; Bhaaganagar and Debnath 2015; Gutierrez et al. 2016; Holtslag 2016; Gutierrez et al. 2017). Therefore, these events require research attention.

Advancements in remote sensing technologies have enabled enhanced measurement of the offshore wind environment. These systems typically measure atmospheric boundary layer (ABL) winds across larger vertical ranges and at greater spatial frequencies than traditional meteorological masts. As part of a meteorological campaign commissioned by the Dutch Ministry of Economic Affairs, multiple measurement platforms located throughout the North Sea have been equipped with remote sensing instruments. These measurements have the potential to lend insight into North Sea anomalous wind event frequency, characteristics, and onset mechanisms.

An anomalous wind event that is of particular interest to the wind energy community is the low-level jet (LLJ). The LLJ is a thin stream of enhanced momentum, typically with wind speeds between 10 m s^{-1} and 20 m s^{-1}, located within the lower portions (i.e. < 300 m) of the ABL (Stull 1988). Onshore LLJs have been observed in Europe (Sladkovic and Kanter 1977; Kraus et al. 1985), Africa (Anderson 1976; Hart et al. 1978), North and South America (Blackadar 1957; Bonner 1968; Lettau 1967), and Australia (Malcher and Kraus 1983; Brook 1985; Garrat 1985). However, relative to the onshore LLJ, less is known regarding offshore LLJ behaviour. Accurately characterising offshore LLJ spatiotemporal behaviour is imperative to ensure future reductions in North Sea wind uncertainty. Therefore, analyses of wind conditions at seven offshore measurement platforms were performed in this study to advance the knowledge and understanding of the offshore LLJ.

This report is structured as follows: section two provides details of the measurement platforms, instruments, and data quality control, section three documents LLJ identification and analysis techniques, and section four provides a discussion of the results.

2 Measurement platforms, instruments, and data quality control

An increasing number of meteorological measurement platforms have been established across the Dutch Part of the North Sea within the last decade in an attempt to provide improved characterisation of the offshore wind environment. Seven of these measurement sites (Figure 1) were used in this study to analyse North Sea LLJ spatiotemporal behaviour. Each station chosen was equipped with light detection and ranging (lidar), and at one location a meteorological mast was also installed. Anemometry specifics and the data quality control procedures employed are detailed in the following sections.

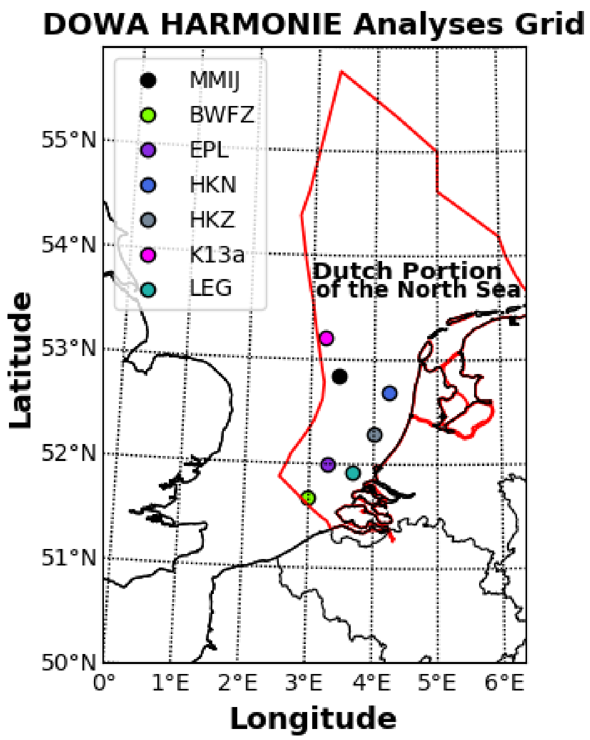

Figure 1. The seven measurement sites used to examine offshore LLJ spatiotemporal behaviour. For identification of the measurement sites, see Table 1.

2.1 Lidar measurements

Vertically pointing lidar provides efficient and non-intrusive measurement of ABL winds. Compared to traditional meteorological masts, lidar typically expand the height and vertical sampling frequency of offshore wind measurements. Although lidar were available at each measurement site, lidar type and mounting procedures varied. Lidar type included the Zephir 300s continuous-wave (CW) lidar and the WINDCUBE v2 pulsed lidar. These lidar were typically platform mounted, except at the Borssele wind farm and Hollandse Kust wind zones (Noord and Zuid) where the lidar was instrumented atop a floating metocean buoy. Also, instead of only one lidar being deployed (such as at measurement locations using platform-mounting procedures), two lidar-equipped metocean buoys were positioned within each of these wind zones.

CW and pulsed wind lidar are coherent systems, meaning they both analyse Doppler shift frequencies to determine an estimate of the radial wind speed (Diaz et al. 2013). However, radial velocity and vertical wind profile extraction techniques differ between the two lidar types. Whereas pulsed wind lidar use range gates to near-simultaneously extract radial velocity estimates at multiple points in space, CW wind lidar can only extract a radial velocity estimate at the beam focus length. This beam focus length must be modified in time in order to measure the wind field at varying locations. The radial wind speed is defined as the motion of the wind towards or away from the remote sensing instrument. Unless the wind is moving along one of these radials, then the wind speed will not be fully resolved. Therefore, CW and pulsed wind lidar use varying adaptations of conical scanning techniques (Banakh et al. 1993) to resolve the horizontal wind field at varying heights above-ground level (AGL). For brevity, these differences are not detailed in this report. However, because of these differences, the vertical wind profile was resolved at 17-s intervals for the CW wind lidar and at 4-s intervals for the pulsed wind lidar. A 10-min average of these vertical wind profiles was used in this study to examine LLJ behaviour.

A summary of the lidar measurements at each site – including lidar type, measurement heights, and the data collection periods – is provided in Table 1. A schematic is also provided in Figure 2 to demonstrate the site-specific measurement heights.

Table 1 Site lidar description. Data collection period start and end times are denoted by the letters S and E. Measurement heights are indicated by HGT_{misc} (if applicable) and HGT_{min}:$HGT_{interval}$:HGT_{max}.

Measurement Location	Lidar Type (x 2 – two site lidars)	Mounting Procedure	Measurement Heights (m)	Data Collection Period
IJmuiden (MMIJ)	ZephIR 300s	Platform-Mounted	90:25:315	S: 11-Nov-2011 E: 09-Mar-2016
Europlatform (EPL)	ZephIR 300s	Platform-Mounted	63, 91:25:291	S: 30-May-2016 E: 31-Dec-2017
Lichteiland Goeree (LEG)	WINDCUBEv2	Platform-Mounted	63, 91:25:291	S: 17-Nov-2014 E: 31-Dec-2017
K13a	ZephIR 300s	Platform-Mounted	63, 91:25:291	S: 01-Nov-2016 E: 31-Mar-2018
Hollandse Kust (Noord) Wind Farm Zone (HKN)	ZephIR 300s x 2 (Sites A and B)	Floating	30, 40, 60:20:200	S: 10-Apr-2017 E: 31-Oct-2017 **Period A = Period B**
Hollandse Kust (Zuid) Wind Farm Zone (HKZ)	ZephIR 300s x 2 (Sites A and B)	Floating	30, 40, 60:20:200	S: 05-Jun-2016 E: 28-Feb 2018 **Period A = Period B**
Borssele Wind Farm Zone (BWFZ)	ZephIR 300s x 2 (Sites I and II)	Floating	30, 40, 60:20:200	**Site I:** S: 11-Jun-2015 E: 27-Feb-2017 **Site II:** S: 12-Feb-2016 E: 07-Jul-2016

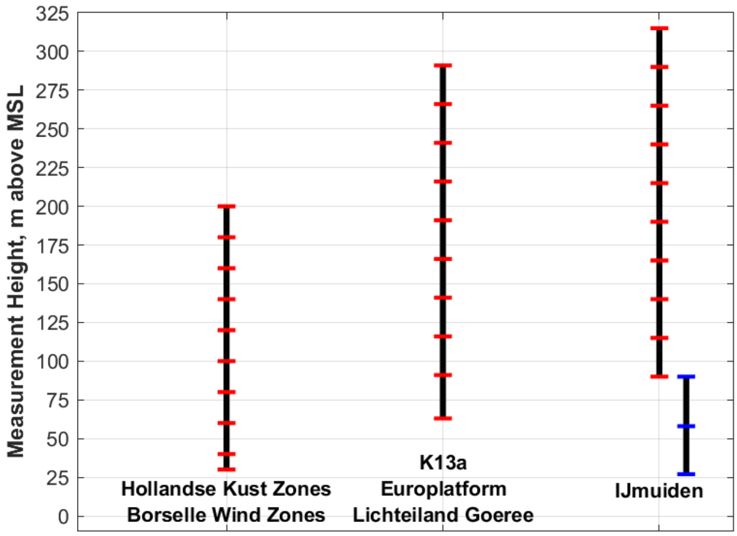

Figure 2. Site-specific lidar (horizontal red lines) and mast (horizontal blue lines) measurement heights.

2.2 Meteorological mast measurements at IJmuiden

Collocated with the wind lidar at MMIJ was a meteorological tower instrumented at multiple levels. Cup anemometry was mounted at 27 m, 58 m, and 85 m to measure horizontal wind speed, and a wind vane was used at 27 m, 58 m, and 87 m to determine the horizontal wind direction. At each measurement level, anemometry was mounted along booms arms at 46.5º (~NE), 166.5º (~SSE), and 286.5º (~WNW). Depending upon the wind direction, tower shading corrections (Werkhoven and Verhoef 2012) were applied to ensure an accurate depiction of the horizontal wind field. In order to couple mast and lidar data, and therefore enable offshore wind analyses between 27 m and 315 m, the lowest lidar and highest mast measurement heights were averaged together. Similar averaging of mast and lidar measurements at MMIJ were performed by Kalverla et al. (2017).

2.3 Data quality control

Data quality control is imperative to ensure an accurate depiction of the offshore LLJ. Implementation of data quality control varied depending upon measurement source (i.e. lidar versus mast) and lidar type (i.e. ZephIR 300s versus WINDCUBE v2). However, considerations were made to ensure data quality control was employed relatively uniformly between measurement sites. At both the Borssele wind farm and Hollandse Kust (Noord and Zuid) wind zones, first-order quality control was already performed by Fugro. An overview of these quality control procedures can be found online (https://offshorewind.rvo.nl).

Regardless of measurement source, plausible value checks were imposed on the wind data. Any 10-min observation that met the following criteria was removed from the data record:

- The mean wind speed was either greater than the period maximum wind speed or less than the period minimum wind speed.
- The mean wind speed was less than 0.05 m s^{-1}.
- Turbulence intensity (TI) for the period fell below 0.10 % (i.e. 0.001).

- At the measurement height, the value of TI was 10 standard deviations (σ_{TI}) greater than the mean (μ_{TI}) TI value (i.e. $TI \geq \mu_{TI} + 10\sigma_{TI}$); μ_{TI} and σ_{TI} were defined as the height-respective value for the entire data collection period. Because TI typically decreases with mean wind speed, this threshold was only imposed if the 10-min mean wind speed exceeded 4 m s^{-1}.

Specific quality control measures were also applied to the lidar wind data. Any 10-min observation that satisfied the following criteria were removed from the data record:

- A lidar error code (e.g. 9998 or 9999) was reported.
- The carrier-to-noise ratio (CNR) was less than -22 (the value of CNR provides a measure of signal strength [i.e. quality]). CNR was only outputted by the WINDCUBE v2 wind lidar.
- Backscatter magnitude was less than $1e^{-5}$ or greater than 100 – backscatter served as a proxy for CNR for data reported by the ZephIR 300s lidar.

Prior analyses (e.g. Poveda and Wouters 2015) demonstrate that the ZephIR 300s lidar can incorrectly measure wind direction by 180°. Analysis of wind data at MMIJ from January 2012 through January 2014 indicated that approximately 3.6 % of the measured wind data exhibited this flow reversal. Although mitigation (i.e. removal) of this data is possible, it requires independent wind direction measurements from a collocated meteorological mast. Because mast data was not available at each site, these wind direction errors were not removed. However, ZephIR 300s lidar wind direction errors did not impact the measured wind speed. Even when the lidar wind direction exhibited this flow reversal error, the measured wind speeds were in agreement with the collocated mast data. This wind direction error was therefore not expected to significantly impact results. However, wind direction sectors were filtered and corresponding data (wind speed and direction) were removed in order to account for the wake effect of neighbouring wind farms. A generous estimate of 20 km was used to denote the maximum wind farm wake length.

3 North Sea LLJ Analyses

3.1 LLJ identification

LLJ identification criteria has often varied between studies. Roughly stated, most studies require a 'significant' wind speed maximum within the lower portions of the vertical wind profile. In this work, the significance of this wind speed maximum was defined relative to the magnitude of a reference minimum wind speed. This reference minimum was defined as the lowest-altitude wind speed minimum that was detected above the wind speed maximum (Figure 3a). However, if at the measurement level above the reference minimum height the wind speed does not increase by at least one meter per second, then this reference minimum was neglected, and the process to determine the reference minimum was continued at higher elevations (Figure 3b). If no sufficient minimum was detected, the wind speed magnitude at the top of the vertical wind profile was used as the reference minimum (Figure 3c). Using thresholds set forth by Baas et al. (2009), a wind profile was classified as a LLJ if the wind speed maximum was at least 2 m s^{-1} and 25 % faster than the reference minimum wind speed. A wind profile was only examined for LLJ presence if the vertical wind profile was fully defined.

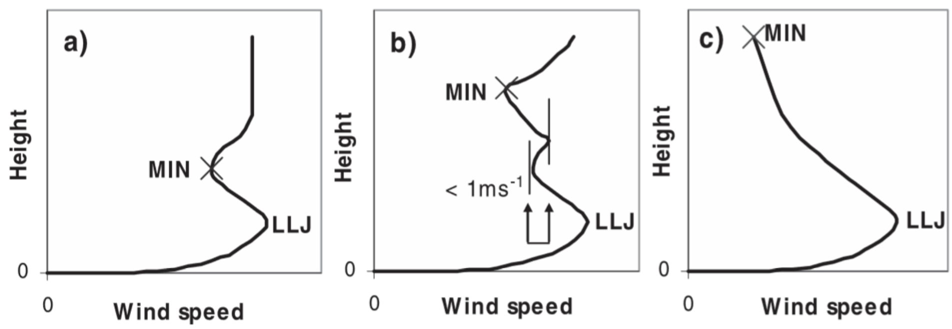

Figure 3. Schematic demonstrating the methods used to determine LLJ maximum and reference minimum velocities. (A) Typically, the reference minimum is the first wind speed minimum detected above the height of the LLJ maximum. (B) However, a wind speed minimum is neglected if, at the measurement level above, there is not at least a one meter per second increase in wind speed. (C) Also, if no sufficient reference minimum can be determined, the wind speed magnitude at the top of the wind profile is used as the reference minimum.

3.2 LLJ profile and event characterisation

Due to the coupling of high-altitude lidar data with low-level mast measurements as well as four-plus years of near-continuous data collection, the most comprehensive measurement of the offshore wind environment occurred at MMIJ. Therefore, MMIJ LLJ characterisation served as the foundation for this report. These results are presented first, followed by LLJ characterisation at other sites and a discussion of factors impacting LLJ characterisation. Analyses conclude with a first-order examination of LLJ spatial coherence.

3.2.1 *MMIJ LLJ characterisation*

High-quality offshore wind measurements at MMIJ, situated about 85 km from the coast, were collected between November 2011 and March 2016. During this period, 228,960 10-min wind profiles were collected. However, approximately 14 % (32,034) of these wind profiles were not considered because the wind profile was not fully defined across the vertical measurement range. Of the remaining 196,926 wind profiles examined, 7,616 (3.87 %) exhibited a LLJ profile. The LLJ wind speed maximum occurred at an average height of 101.51 m with a mean velocity of 9.28 m s^{-1} (Figure 4). The value of the LLJ wind speed maximum was on average 83.72 % greater than the reference minimum wind speed at 279.85 m. This provides an indication of the inverse shear present above the LLJ maximum.

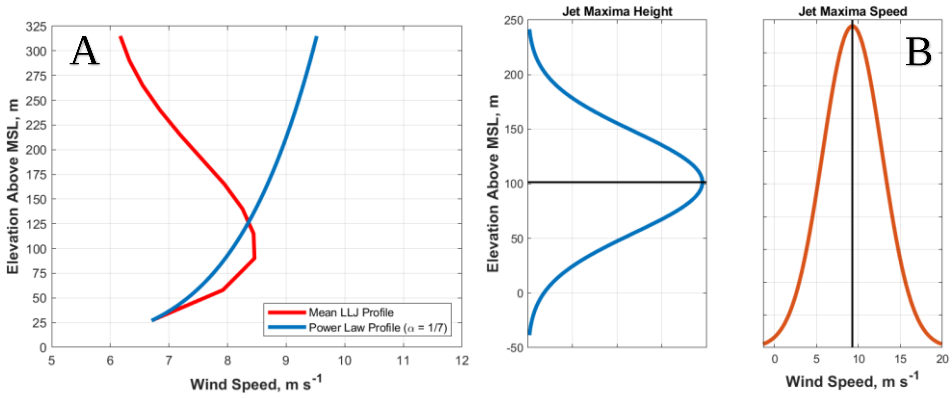

Figure 4. (A) The mean LLJ wind profile (red line) overlaid by a power-law wind profile (blue line) with an assumed alpha value of 1/7. (B) Kernel estimate of the probability density function of LLJ maxima height (blue line) and wind speed (red line).

LLJ occurrence varied with wind direction (Figure 5a). LLJ occurrence as a function of wind direction sector was approximately: (1) 30 % between 0º and 90º (i.e. Q1), (2) 25 % between 90º and 180º (i.e. Q2), (3) 34 % between 180º and 270º (i.e. Q3), and (4) 11 % between 270º and 360º (i.e. Q4). The relative occurrence percentages provided are defined relative to all of the measured wind data, regardless of wind direction sector (i.e. Q1, Q2, Q3, Q4). Therefore, although LLJ occurrence was highest with winds from the southwest, this did not indicate that southwest winds were more likely than other wind directions to contain a LLJ. Southwest winds were most common at MMIJ (Figure 5b); therefore, it is trivial that a LLJ would emanate most often from this wind direction. Considering the frequency distribution of both MMIJ LLJ occurrence and wind direction, the highest probability of LLJ occurrence was actually with northerly winds. LLJ maxima height and velocity also varied as a function of wind direction (Figure 6). The strongest LLJs – as defined by the jet maxima wind speed – were observed with winds from the southwest. Analysis of LLJ profile shape as a function of wind direction suggests a direct relationship between LLJ maxima height and strength. Although not examined here, a more thorough analysis of this relationship might be of benefit to the wind engineering community.

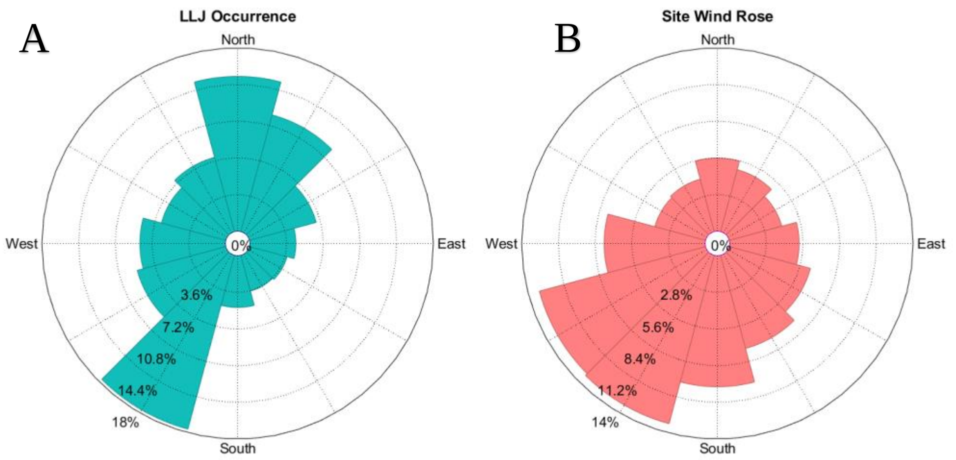

Figure 5. (A) MMIJ LLJ occurrence as a function of wind direction and (B) the MMIJ wind rose.

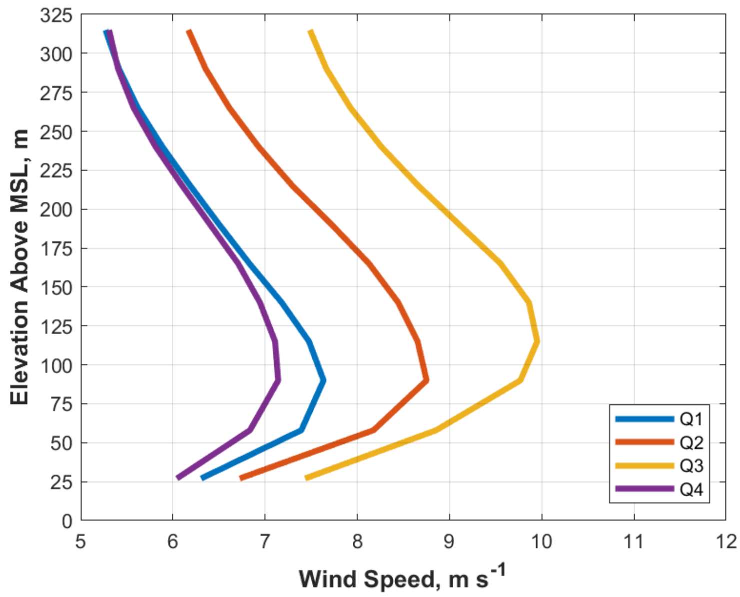

Figure 6. Mean LLJ wind profile as a function of wind direction sector. Wind direction sectors (i.e. Q1, Q2, Q3, Q4) are defined in text.

The annual LLJ occurrence rate of 3.87 % does not accurately depict LLJ likelihood at any point during the year. Seasonal variability in atmospheric conditions means that during some seasons – i.e. spring (calendar months: MAM) and summer (calendar months: JJA) – LLJ incidence was amplified, whereas in other seasons – i.e. fall (calendar months: SON) and winter (calendar months: DJF) – LLJ occurrence was diminished. For the four-plus year period analysed, summer winds contained a LLJ 7.56 % of the time, and spring winds contained a LLJ 6.61 % of the time. LLJ frequency within the fall was reduced to 1.30 %, and similarly was reduced to 1.05 % within the winter. Seasonal differences in LLJ frequency followed trends in ABL stability. This was demonstrated by examining the season-respective magnitude of the virtual potential temperature gradient $\Delta\theta_V$ (Figure 7a). Positive values of $\Delta\theta_V$ are indicative of a stable ABL, whereas negative values suggest a convective, or unstable, ABL. Large magnitude positive $\Delta\theta_V$ values indicating stable conditions were most commonly observed within the spring and summer months. This supports the hypotheses that LLJs are fostered by stable conditions (e.g. Angevine et al. 2006; Dörenkämper et al. 2015; Kalverla et al. 2017), which can occur across the North

Sea when warm continental air is advected over the cooler ocean. Seasonal mean LLJ wind profiles are provided in Figure 7b.

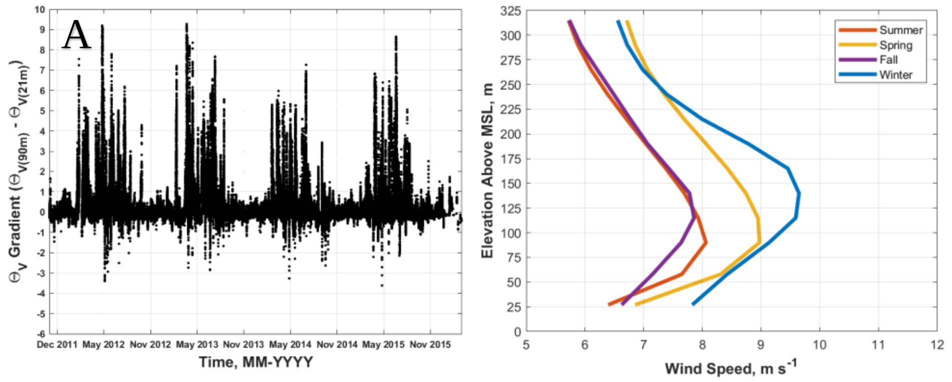

Figure 7. (A) The vertical θ_V graident between 90 m and 21 m (i.e. $\theta_{V|90m|} - \theta_{V|21m|}$). (B) Mean LLJ wind profile as a function of seasonal cycle.

Inter-site comparison of the offshore LLJ in order to examine LLJ spatial variation was a principal focus of this work. However, data collection at the various measurement sites was not concurrent. Therefore, it was important to determine how LLJ characteristics vary at a single location with time in order to denote whether inter-site comparison of the offshore LLJ was appropriate. Although interannual differences in LLJ behaviour existed at MMIJ, distinct trends (i.e. increasing or decreasing) in LLJ occurrence (Figure 8a), LLJ maxima height (Figure 8b [blue circles]), and LLJ maxima wind speed (Figure 8b [orange circles]) were not observed between 2012 and 2015. Data from 2011 and 2016 were not considered because they did not encompass a full calendar year of measurements (i.e. Jan – Dec). LLJ annual occurrence peaked at 5.28 % in 2013, and in 2012 reached a minimum value of 3.05 %. Annual average LLJ maxima height varied between 91.45 m and 105.98 m, and the annual average LLJ maxima wind speed varied between 8.90 m s^{-1} and 9.79 m s^{-1}. It was difficult to discern whether these changes were due to interannual LLJ variability or interannual differences in seasonal data availability. Therefore, although interannual differences in LLJ behaviour were minimal, inter-site LLJ comparisons should be performed with caution; emphasis should be placed on seasonal as opposed to annual inter-site comparisons.

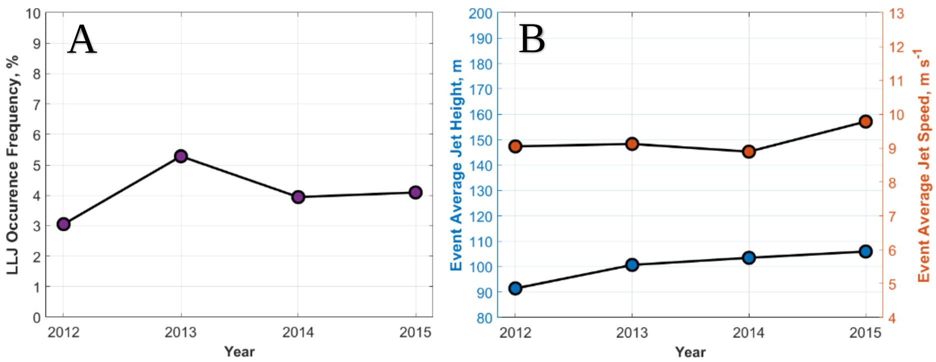

Figure 8. (A) Annual average time history of (A) LLJ occurrence and (B) LLJ maxima height (blue circles) and wind speed (orange circles).

3.2.2 *MMIJ LLJ event temporal analysis*

In order to examine LLJ temporal behaviour, research has primarily examined LLJ occurrence as a function of the diurnal cycle (e.g. Marengo et al. 2004; Song et al. 2005; Karipot et al. 2009; Rijo et al. 2018). This research indicates LLJ tendency to form during the night, but does not give any indication of LLJ temporal persistence. Even research that has explicitly noted persistence in the LLJ (Vanderwende et al. 2015) has not provided quantitative methods to examine this temporal persistence. To address this issue, a framework was established in this study to systematically identify persistent LLJs (i.e. LLJ events) so that LLJ temporal behaviour could be quantitatively analysed.

The following methods were used to determine LLJ event initiation and cessation. LLJ event initiation (i.e. onset time) occurred when at least two 10-min wind profiles within a 30-min period satisfied the criteria for a LLJ. Once LLJ event initiation occurred, this 30-min window was advanced in time until there were zero LLJ wind profiles within the 30-min period, thereby denoting LLJ event cessation. LLJ event duration was defined as the time period between the first and last LLJ profiles detected. Demonstrating the robustness of the technique and LLJ wind profile persistence, only 510 (6.7 %) of the 7,616 LLJ profiles identified at MMIJ were not contained within a LLJ event. The thresholds presented in this report represent a first-order attempt to identify LLJ events, and therefore are not expected to comprehensively resolve this phenomenon. A thorough sensitivity analysis should be performed in future work to determine LLJ event sensitivity to the chosen parameters. Also, parameter selection will need to be modified to accommodate varying wind speed averaging periods.

LLJ events at MMIJ typically initiated at 00:10 UTC and lasted for 96.6 min. A non-parametric kernel density estimator with bounded support was used to define the probability density function for both LLJ event onset time (Figure 9a) and duration (Figure 9b). The distribution of LLJ event onset times exhibited a peak during the night with LLJ event onset frequency diminishing towards the tails (i.e. the daytime period). Alternatively, the LLJ event duration distribution was heavy-tailed with a positive skew. More than half (51.5%) of the LLJ events identified exceeded one hour in duration; six of these events persisted for more than 10 hrs. A maximum LLJ event duration of 27 hrs was detected. Also, LLJ event duration did not exhibit considerable variation as a function of LLJ event onset time (Figure 10).

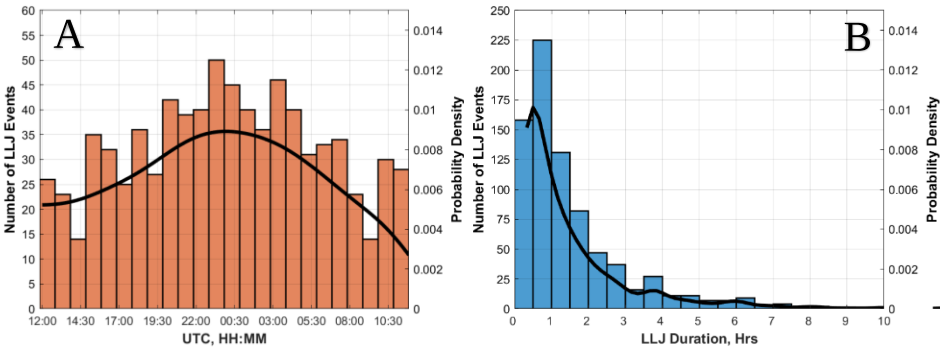

Figure 9. Histogram of both LLJ event (A) onset time and (B) duration overlaid by the respective kernel estimate of the probabiltiy density function.

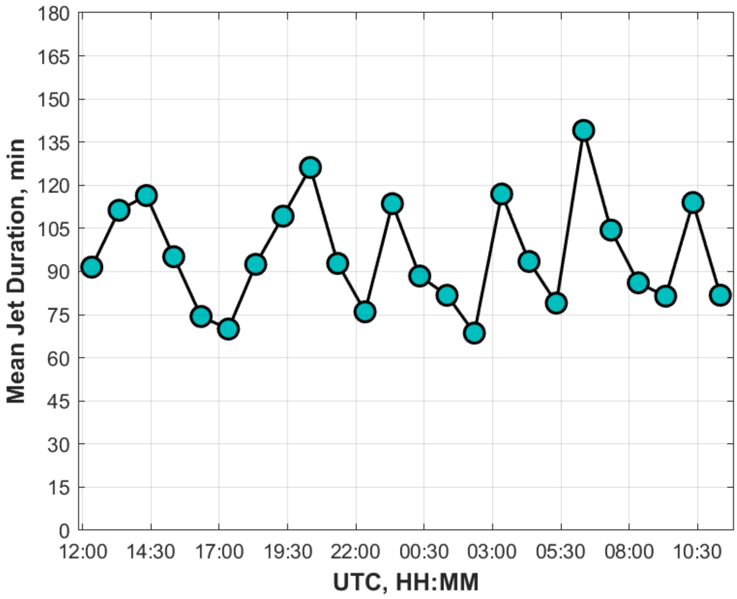

Figure 10. Mean LLJ event duration as a function of event onset time.

Both LLJ event onset time and duration exhibited seasonal variability. LLJ events in the spring initiated slightly before those in the fall, which initiated slightly before those in the summer (Figure 11). Within the winter a strong peak in LLJ event initiation time did not occur; the winter LLJ event onset time distribution was relatively flat throughout the night. The longest LLJ events occurred in the spring and summer months. Summer LLJs exhibited a mean duration of 99.2 min, whereas spring LLJs typically persisted for an average time of 105.7 min. Mean LLJ event duration was reduced to 77.1 min in the winter and 69.9 min in the fall. Spring and summer months also saw more than double the number of three-plus hour LLJ events than those observed in the fall and winter months.

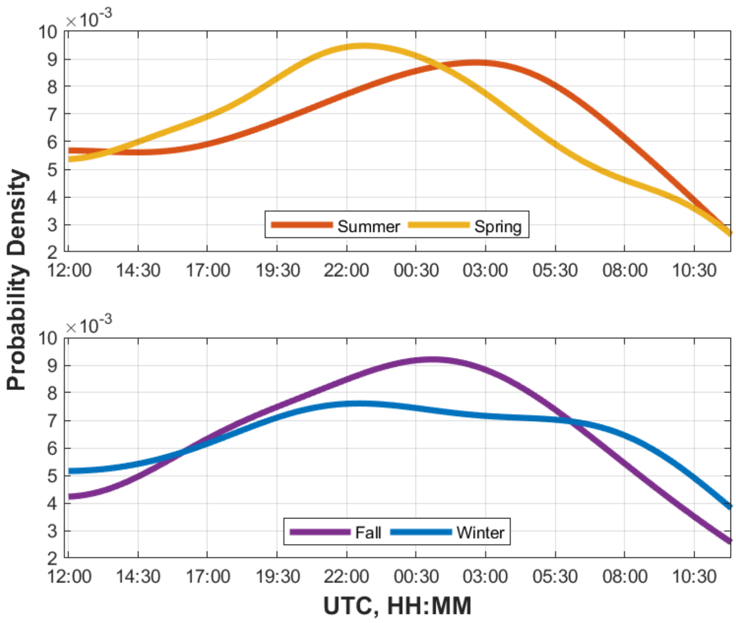

Figure 11. Kernel density estimate of seasonal LLJ event initiation time.

3.2.3 *MMIJ LLJ intra-event profile evolution*

The focus of segmenting LLJ wind profiles into larger-scale events was to enable quantitative analysis of LLJ temporal behaviour. However, defining these events also enables the examination of wind and atmospheric conditions before, within, and following these events. Wind speed evolution within a typical one-hr LLJ event at MMIJ is shown in Figure 12a. Wind analysis techniques can further be modified to examine intra-event evolution of wind shear (Figure 12b) and veer (Figure 12c). Values of wind shear and veer provided in Figure 12 were defined as the difference in wind measurement (i.e. wind speed or direction) between 27 m and the subsequent measurement height (i.e. $Wind_{27m} - Wind_{XXm}$). Although this analysis topic is presented, an in-depth examination of intra-event wind evolution was not performed. For future work, it would be interesting to note how LLJ wind profiles vary within larger-scale temporal events such as the 27 hr LLJ event observed at MMIJ.

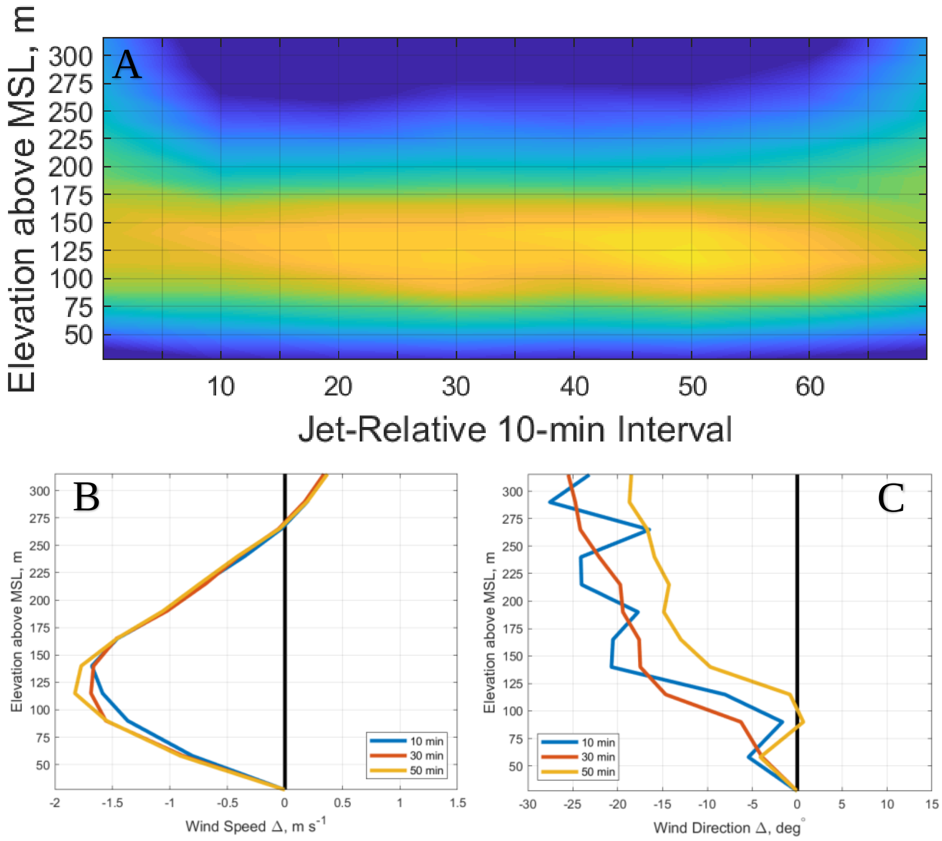

Figure 12. (A) LLJ wind profile evolution within a one-hour LLJ event along with corresponding profiles of wind (B) shear and (C) veer at event-relative intervals of 10-min, 30-min, and 50-min.

3.3 North Sea LLJ spatial variability

Expanding LLJ analyses to other portions of the North Sea that will see future wind farm development (i.e. Figure 13) is imperative to reduce offshore wind resource uncertainty. LLJ identification criteria was therefore applied to wind data from each available measurement site to examine spatial differences in LLJ behaviour. Site-specific LLJ occurrence and wind profile characteristics (summarized in Table 2) exhibited sensitivity to site measurement height, which was dictated by the lidar capabilities and site mounting procedures. Lidar at MMIJ, EPL, and K13a were able to measure higher altitudes winds than those at BWFZ, HKN, and HKZ. Those stations that measured at higher altitudes detected a higher occurrence of LLJs. LLJ detection sensitivity to site measurement height can be partially attributed to the impact of measurement height on the reference minimum value chosen. If wind speeds steadily decrease with altitude or if a sufficient wind speed minimum was not determined (i.e. Figure 3c), then the wind speed at the top of the wind profile was used as the reference minimum value. Those stations that measure at higher altitudes will therefore demonstrate a propensity to detect lower magnitude reference minimum values, which should increase the likelihood of LLJ detection. Alternatively, sites that measure at higher altitudes might not properly resolve LLJ maxima occurring below the lowest lidar measurement height of 90 m. LLJ maxima height and strength will therefore also be sensitive to site measurement height. This research suggests that a deep vertical measurement range is required to comprehensively analyse offshore LLJ behaviour, and further that a uniform vertical measurement range is required for equivalent inter-site LLJ comparison. An overview of spatial variation in LLJ temporal behaviour is provided in Table 3. However, because inter-site comparison of LLJ behaviour was hindered by differences in site measurement height and non-concurrent data collection periods (Figure 14), further discussion of LLJ spatial variability was not provided.

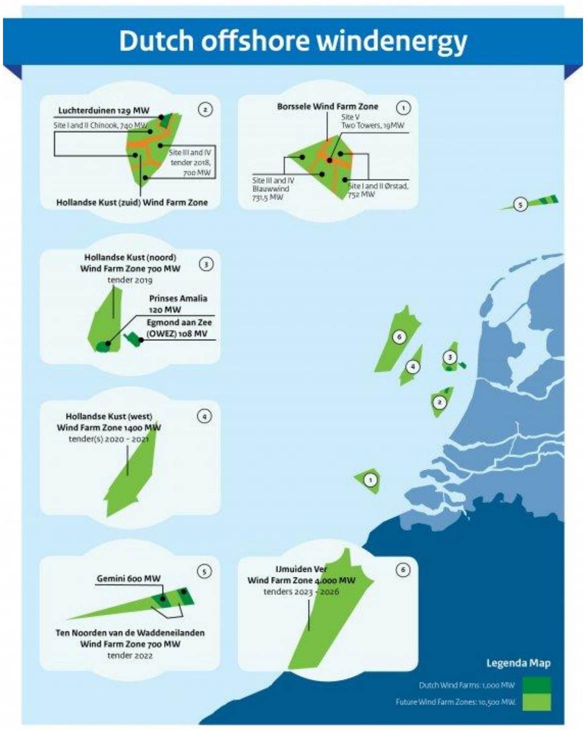

Figure 13. Offshore wind energy roadmap that outlines future wind farm development regions (image provided by: https://www.rvo.nl).

Table 2 Site-specific LLJ frequency and general profile characteristics – results are parsed relative to the site-specific measurement range.

Site Measurement Range 90 m – 291 m	Wind Speed Profiles Examined	LLJ Profile Detection (%)	LLJ Maxima Mean Wind Speed (m s^{-1})	LLJ Maxima Mean Height (m)
MMIJ (lidar data only)	215,942	2.89	9.53	115.6
LEG	76,058	2.57	8.32	120.5
EPL	80,289	3.21	8.94	113.8
K13a	73,922	2.43	9.65	122.8
Site Measurement Range 27 m – 215 m				
MMIJ (lidar and mast data)	197,415	2.12	8.42	80.6
Hollandse Kust Noord (A)	18,659	1.18	7.10	60.7
Hollandse Kust Noord (B)	21,273	1.31	7.14	54.9
Hollandse Kust Zuid (A)	76,534	0.77	7.53	69.1
Hollandse Kust Zuid (B)	79,048	0.76	7.58	67.2
Borssele Wind Farm Zone (Site 1)	37,028	2.79	8.45	65.7
Borssele Wind Farm Zone (Site 2)	8,939	5.01	9.18	71.7

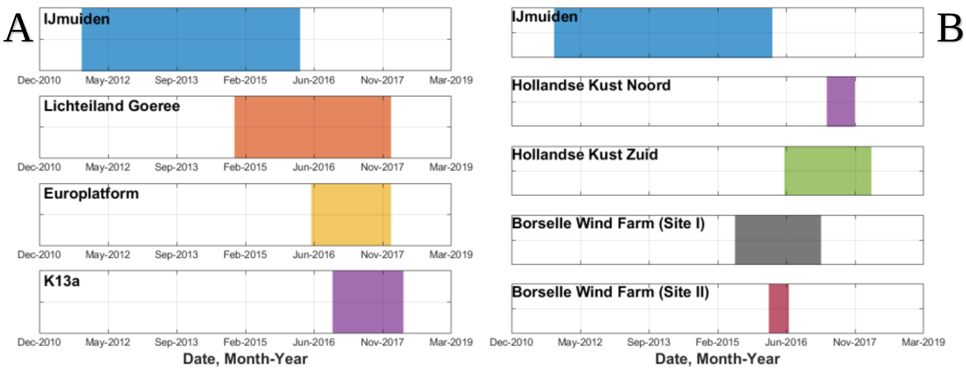

Figure 14. Data collection periods for those stations with measurements occurring between (A) 90 m and 291 m and (B) 27 m and 215 m.

Table 3 Site-specific LLJ event temporal behaviour – results are parsed relative to the site-specific measurement range.

Site-Specific Measurement Range: 90 m – 291 m	Number of LLJ Events Identified	Mean LLJ Event Onset Time (UTC)	Mean LLJ Event Duration (mins)	Number of LLJ Events in Excess of 10 Hrs
MMIJ (lidar data only)	696	00:00	90.1	4
LEG	210	00:40	90.1	2
EPL	295	00:00	86.4	1
K13a	234	00:00	75.3	0
Site-Specific Measurement Range: 27 m – 215 m				
MMIJ (lidar and mast data)	450	00:10	92.5	3
Hollandse Kust Noord (A)	25	22:10	89.6	0
Hollandse Kust Noord (B)	36	21:20	80.3	0
Hollandse Kust Zuid (A)	89	01:10	59.7	0

Hollandse Kust Zuid (B)	97	00:50	57.2	0
Borssele Wind Farm Zone (Site 1)	110	23:30	96.6	0
Borssele Wind Farm Zone (Site 2)	37	22:20	123.5	1

3.3.1 LLJ spatial coherence

Inter-site comparison of the offshore LLJ was hindered by many factors. Therefore, different analysis techniques were developed to examine offshore LLJ spatial coherence. Analyses of LLJ behaviour at measurement site pairs (i.e. Site A and B) that exhibited extended periods of concurrent data collection were used to investigate the following question. If a LLJ was detected at Site A, what was the probability that a LLJ would be detected at a neighbouring Site B, and at what time lag (i.e. Site A LLJ detection time + XX hrs) does this detection typically occur? This analysis lends insight into whether LLJs are isolated North Sea events, or whether they constitute some larger scale atmospheric phenomenon as suggested in literature.

Analysis was performed between measurement platforms K13a (Figure 15a [blue circle]) and EPL (Figure 15a [red circle]) and LEG (Figure 15a [yellow circle]) and EPL. Measurement platform EPL was located about 135.6 km to the south-southeast of K13a, and approximately 28.4 km to the northwest of LEG. Measurement platform spatial distribution enables rough analysis of north-south, and to a lesser degree east-west, LLJ spatial coherence. When a LLJ was identified at either site (e.g. Site A), then wind conditions at the neighbouring site (e.g. Site B) were analysed to investigate whether the wind conditions there also satisfied the criteria for a LLJ. Site B wind conditions were initially examined for the one-hr time period following Site A LLJ detection. If a LLJ wind profile was detected within this time interval, analysis ended and the time lag (i.e. one hour) was noted. However, if no LLJs were detected within the time period, then the search window was expanded by one hour and the LLJ search process was repeated. This analysis was iterated outwards of 24 hrs or until a LLJ wind profile was detected at Site B. Analysis was only performed if at least 75 % of the wind profiles within the search interval were fully defined.

When a LLJ was detected at either K13a or EPL, there was a high probability (>70 %) of LLJ occurrence at the neighbouring site within 24 hrs (Figure 15b). Similar patterns were observed between LEG and EPL, wherein an even higher likelihood (>80 %) of LLJ detection at the neighbouring measurement site was noted at the end of the 24-hr period (Figure 15c). Given the distance between measurement sites, it makes sense that initial LLJ detection rates were higher for the measurement pair LEG and EPL (~ 50 %) than for K13a and EPL (~ 25 %). Also, the probability of LLJ occurrence at EPL (given a LLJ was detected at LEG) did not significantly differ from the probability of LLJ occurrence at LEG (given a LLJ was detected at EPL). Again, this makes sense given the close proximity of the measurement stations to one another. However, between measurement pair K13a and EPL, the probability of LLJ detection at the neighbouring site was consistently larger when the LLJ was first identified at K13a. This could indicate that offshore LLJs typically form in the north before propagating south. Further explanation of the physical mechanisms that govern this southward propagation is outside the scope of this work. In closing, the high-likelihood of LLJ occurrence at neighbouring measurement locations when a LLJ profile was detected at a given site supports North Sea LLJ spatial coherence. Subsequent work should leverage similar techniques to determine North Sea LLJ spatial propagation patterns, which might lend insight into the physical mechanisms governing North Sea LLJ behaviour.

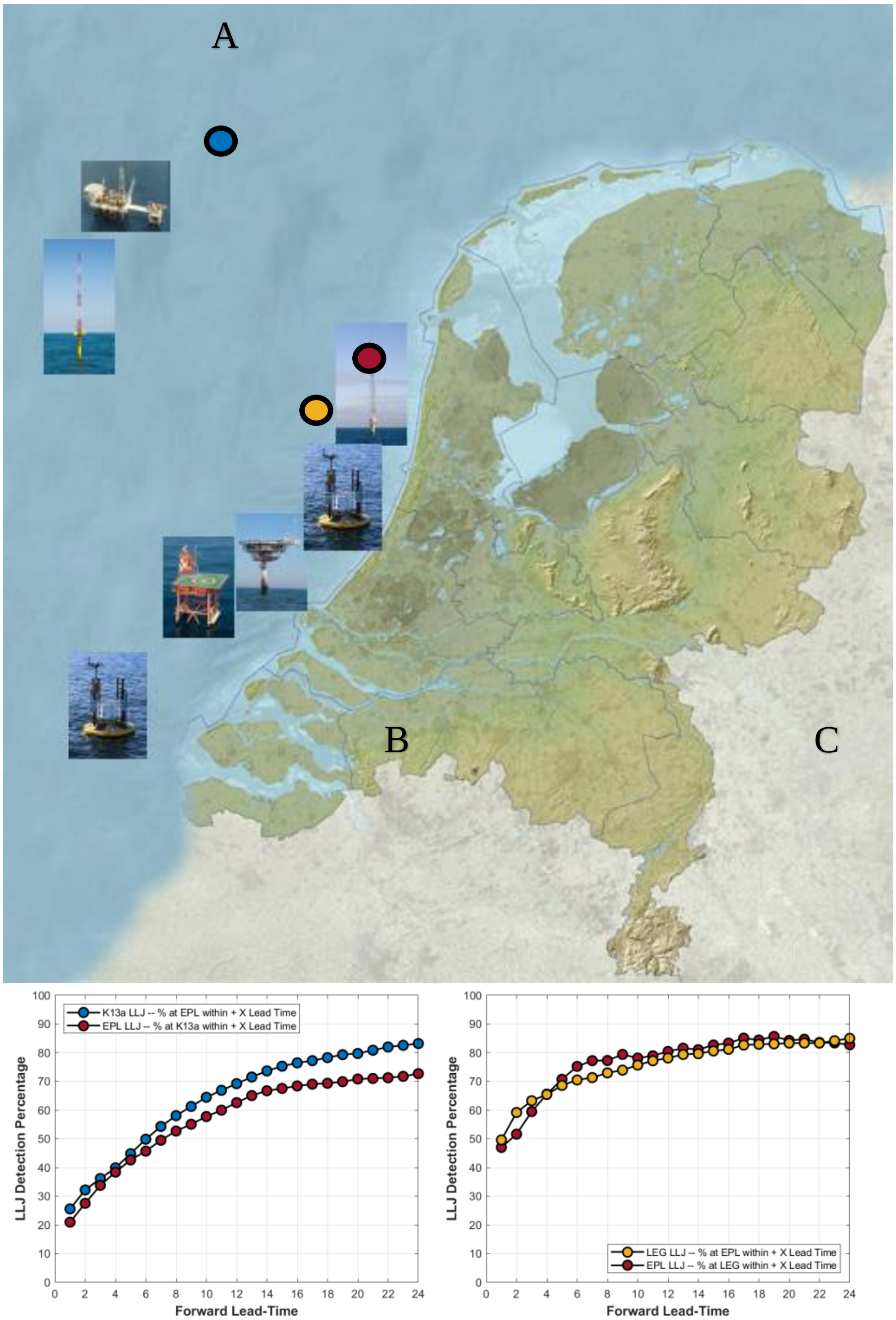

Figure 15. (A) The spatial distribution of North Sea measurement sites – measurement sites used in analysis are overlaid by a colored circle (colors are defined in text). The likelihood of LLJ detection at the neighbouring measurement site for measurement pairs (B) K13a and EPL and (C) LEG and EPL.

4 Concluding remarks and discussion

Due to historically limited measurement of the offshore ABL, especially at high altitudes, uncertainty in offshore wind remains. Although numerical weather models can reasonably resolve mean wind conditions, less is known regarding the behaviour of the offshore LLJ – an anomalous wind event that can significantly impact both wind turbine power performance and loading. In order to ensure future wind farm effectiveness, it is paramount that the North Sea LLJ is thoroughly characterized. Therefore, using wind data from seven offshore measurement platforms, the focus of this work was to improve spatiotemporal characterisation of the North Sea LLJ.

Analyses of North Sea wind conditions at these measurement platforms indicate that LLJ wind profile occurrence is not rare. A LLJ wind profile at MMIJ was detected 3.87 % of the time with the LLJ maxima occurring at an average height of 101.51 m with a mean wind speed of 9.28 m s^{-1}. These LLJ maxima height and wind speed characteristics were similar to what has been observed onshore (Banta et al. 2002). LLJ frequency and jet maxima characteristics were both seasonally and directionally dependent. LLJ occurrence was amplified during the spring and summer with winds emanating from the south-southwest. However, this directional peak in LLJ occurrence was due to site climatology as winds emanated heavily from quadrant three. The probability that a given wind profile satisfies the criteria for a LLJ was actually greatest with winds from the north to north-northeast. Also established in this work were novel methods to discern LLJ events, which enabled quantitative analyses of LLJ temporal behaviour (i.e. onset time and duration). These events typically initiated during the night (~ 00:10 UTC) at MMIJ and on average persisted for 96.6 min. The distribution of LLJ event duration times was heavy-tailed (positive skew) with several LLJ events lasting in excess of 10 hrs. A maximum duration time of 27 hrs was detected. Similar to LLJ profile frequency, LLJ event duration was also seasonally dependent. The longest LLJ events occurred in spring and summer, whereas event duration was significantly reduced in the fall and winter. However, regardless of season, LLJ event onset remained greatest during the night.

Identifying LLJ sensitivity to seasonal cycle, wind direction, and vertical measurement range was a significant finding of this work. Measurement sites sampling across larger vertical ranges and at higher altitudes typically detected a greater percentage of LLJs. Sites sampling at higher altitudes also denoted increased LLJ maxima wind speed and height. Knowledge of these sensitivities informs researchers when direct inter-site comparison of LLJ behaviour is appropriate. Appropriate inter-site comparison of LLJ behaviour not only requires uniform LLJ detection criteria and seasonally concurrent data collection periods, but also similar vertical measurement profiles.

Inter-site comparison of LLJ behaviour was not appropriate for many of the available measurement sites. However, because knowledge of offshore LLJ spatial coherence is paramount, alternative analysis techniques were established to explore offshore LLJ spatial variability. Analyses of LLJ frequency and timing at measurement sites K13a, EPL, and LEG suggest that if a LLJ wind profile is detected at a given site, then there is a high probability (i.e. > 70 %) of LLJ detection at a neighbouring site within a 24-hr period. Further research is needed to determine whether the same LLJ is responsible for detection at neighbouring measurement sites – i.e. does the

LLJ propagate with space and time? Regardless, these percentages support theory that LLJs are not isolated or spurious events, but rather are spatially widespread and can occupy a significant area.

4.1 Recommendations for future work

This work lent insight into offshore LLJ frequency and jet maxima height and intensity at various North Sea locations. These results indicate, as prior research has, that LLJs have the potential to impact wind turbine performance. While results demonstrated that LLJ maxima occur within rotor sweep of a typical offshore wind turbine, it is unsure whether there is a net increase or decrease in the mass flux across the rotor sweep. Future analyses should examine the change in wind turbine rotor sweep mass flux in order to quantify the potential benefit or harm of LLJs to wind turbine power performance. Additionally, a more systematic and quantitative approach should be taken to examine changes in wind shear, veer, and vertical profiles of both TI and turbulence kinetic energy that occur in the presence of LLJs. These vertical profile modifications likely reside outside the design specifications of offshore wind turbines, and therefore can significantly impact wind turbine loading characteristics. Examining these things will allow researchers to better quantify the potential impacts of the offshore LLJ on wind turbine performance and efficiency.

In order to better understand LLJ spatiotemporal behaviour and the potential onset mechanisms of offshore LLJs, greater temporal overlap (i.e. concurrent data collection) between the various measurement sites must be established. Once these quality datasets have been developed, analysis techniques should be re-applied so that the propagation patterns of North Sea LLJs can be better analysed. This should lend insight into the physical mechanisms that govern these anomalous wind events, and further might allow researchers to apply some sort of measure-correlate-predict methodologies to this event. While methods were established to examine LLJ temporal behaviour on a first-order basis, a thorough sensitivity analyses should be performed on the various parameters that were used to denote LLJ event initiation and cessation. A more thorough literature search should also be performed on extreme value theory to see what other techniques might be available to quantify LLJ event persistence. Also, in order to gain a more comprehensive understanding of these offshore LLJ events, wind and general atmospheric conditions before, during, and after these events should be examined.

4.2 Acknowledgements

This report was supported with Topsector Energy subsidy from the Ministry of Economic Affairs and Climate Policy.

5 References

Anderson, D. L. T., 1976: The low-level jet as a western boundary current. *Mon. Wea. Rev.*, **104**, 907-921.

Angevine, W. M., J. E. Hare, C. W. Fairall, D. E. Wolfe, R. J. Hill, W. A. Brewer, and A. B. White, 2006: Structure and formation of the highly stable marine boundary layer over the Gulf of Maine. *J. Geophys. Res.*, **111**, D23S22.

Baas, P., F. C. Bosveld, H. Klein Baltink, and A. A. M. Holtslag, 2009: A climatology of nocturnal low-level jets at Cabauw. *J. Appl. Meteorol. Climatol.*, **48**, 1627-1642.

Banakh, V. A, I. N. Smalikho, F. Köpp, and C. Werner, 1993: Representativeness of wind measurements with CW Doppler lidar in the atmospheric boundary layer. *Appl. Opt.*, **34**, 2055-2067.

Banta, R. M., R. K. Newsom, J. K. Lundquist, Y. L. Pichugina, R. L. Coulter, and L. Mahrt, 2002: Nocturnal low-level jet characteristics over Kansas during CASES-99. *Bound.-Layer Meteorol.*, **105**, 221-252.

Bhaganagar, K., and M. Debnath, 2015: The effects of mean atmospheric forcings of the stable atmospheric boundary layer on wind turbine wake. *J. Renew. Sustain. Energ.*, **7**, 013124.

Blackadar, A. K., 1957: Boundary layer wind maxima and their significance for the growth of nocturnal inversions. *Bull. Amer. Meteorol. Soc.*, **38**, 283-290.

Bonner, W. D., 1968: Climatology of the low-level jet. *Mon. Wea. Rev.*, **96**, 833-850.

Brook, R. R., 1985: Koorin nocturnal low-level jet. *Bound.-Layer Meteorol.*, **32**, 133-154.

Brown, A. R., A. C. M. Beljaars, H. Hersbach, A. Hollingsworth, M. Miller, and D. Vasiljevic, 2005: Wind turning across the marine atmospheric boundary layer. *Q. J. R. Meteorol. Soc.*, **131**, 1233-1250.

Burton, T., N. Jenkins, D. Sharpe, and E. Bossanyi, 2011: Wind energy handbook: second edition. John Wiley & Sons, Ltd., Chichester, UK.

Diaz, P. and coauthors, 2013: Remote sensing for wind energy. DTU Wind Energy. (DTU Wind Energy E; No. 0029).

Dörenkämper, M. M. Optis, A. Monahan, and G. Steinfeld, 2015: On the offshore advection of boundary-layer strucutres and the influence on offshore wind conditions. *Bound.-Layer Meteorol.*, **155**, 549-482.

Garratt, J. R., 1985: Inland boundary layer at low latitudes. Part 1, the nocturnal jet. *Bound.-Layer Meteorol.*, **32**, 307-327.

Gutierrez, W., G. Araya, P. Kiliyanpilakkil, A. Ruiz-Columbie, M. Tutkun, and L. Castillo, 2016: Structural impact assessment of low-level jets over wind turbines. *J. Renew. Sustain. Energ.* **8**, 023308.

Gutierrez, W., A. Ruiz-Columbie, M. Tutkun, and L. Castillo, 2017: Impacts of the low-level jet's negative wind shear on the wind turbine. *Wind Energ. Sci.*, **2**, 533-545.

Hart, J. E., G. V. Rao, H. van de Boogaard, J. A. Young, and J. Findlater, 1978: Aerial observations of the E. African low-level jet stream. *Mon. Wea. Rev.*, **106**, 1714-1724.

Holtslag, M. C., 2016: Far offshore wind conditions in scope of wind energy. Ph.D. Dissertation, TU Delft.

Kalverla, P. C., G. J. Steeneveld, R. J. Ronda, and A. A. M. Holtslag, 2017: An observational climatology of anomalous wind events at offshore meteomast IJmuiden (North Sea). *J. Wind Eng. Ind. Aerodyn.*, **165**, 86-99.

Karipot, A., M. Y. Leclerc, and G. Zhang, 2009: Characteristics of nocturnal low-level jets observed in the North Florida area. *Mon. Wea. Rev.*, **137**, 2605-2621.

Kraus, H., J. Malcher, and E. Schaller, 1985: Nocturnal low-level jet during PUKK. *Bound.-Layer Meteorol.*, **31**, 187-195.

Lettau, H. H., 1967: Small to large scale features of boundary layer structure over mountain slopes. *Proc. Symp. On Mountain Meteorol.*, Colorado State Univ., Ft. Collins, Part 2. 1-74.

Malcher, J., and H. Kraus, 1983: Low-level jet phenomena described by an integrated dynamic PBL model. *Bound-Layer Meteorol.*, **27**, 327-343.

Marengo, J. A., W. R. Soares, C. Saulo, and M. Nicolini, 2004: Climatology of the low-level jet east of the Andes as derived from the NCEP-NCAR Reanalyses: Characteristics and temporal variability. *J. Climatol.*, **17**, 2261-2280.

Mirocha, J. D., M. D. Simpson, J. D. Fast, L. K. Berg, and R. L. Baskett, 2016: Investigation of boundary-layer wind predictions during nocturnal low-level jet events using the Weather Research and Forecasting model. *Wind Energ.*, **19**, 739-762.

Park, J., S. B. and L. Manuel, 2014: Large-eddy simulation of stable boundary layer turbulence and estimation of associated turbine loads. *Wind Energ*., **17**, 359-384.

Poveda, M., and D. Wouters, 2015: Wind measurements at meteorological mast IJmuide. ECN-Wind, Report-14-058, ECN, Petten, NL.

Rijo, N., A. Semedo, P. M. A. Miranda, D. Lima, R. M. Cardoso, and P. M. M. Soares, 2018: Spatial and temporal variability of the Iberian Peninsula coastal low-level jet. *Int. J. Climatol.*, **38**, 1605-1622.

Sladkovic, R., and H. J. Knator, 1977: Low-level jet in the Bavarian pre-alpine regime. *Arch. Met. Geoph. Biokl.*, **25**, 343-355.

Song, J., K. Liao, R. L. Coulter, and B. M. Lesht, 2005: Climatology of the low-level jet at the southern great plains atmospheric boundary layer experiment site. *J. Appl. Meteorol.*, **44**, 1593-1606.

Stull, R. B., 1988: An introduction to boundary layer meteorology. Spring, Dordrecht, Netherlands.

Vanderwende, B. J., J. K. Lundquist, and M. E. Rhodes, 2015: Observing and simulating the summertime low-level jet in Central Iowa. *Mon. Wea. Rev.*, **143**, 2319-2336.

Werkhoven, E. J., and J. P. Verhoef, 2012: Offshroe meteorological mast Ijmuiden – Abstract of instrumentation report. ECN-Wind, Memo-12-010, ECN, Petten, NL.

6 Signature

Petten, <datum> TNO

<naam afdelingshoofd>
Head of department

J. B. Duncan
Author